Published in final edited form as:
Biochem Pharmacol. 2009 September 15; 78(6): 648–655. doi:10.1016/j.bcp.2009.05.012.

Ethanol selectively impairs clathrin-mediated internalization in polarized hepatic cells

David J. Fernandez[a], **Benita L. McVicker**[b], **Dean J. Tuma**[b], and **Pamela L. Tuma**[a]

[a] Department of Biology, The Catholic University of America, Washington DC, 20064

[b] Department of Internal Medicine, University of Nebraska, Omaha, NE, 68105

Abstract

Although alcoholic liver disease is clinically well-described, the molecular basis for alcohol-induced hepatotoxicity is not well understood. Previously, we determined that the clathrin-mediated internalization of asialoglycoprotein receptor was impaired in ethanol-treated WIF-B cells whereas the internalization of a glycophosphatidylinositol-anchored protein thought to be endocytosed via a caveolae/raft-mediated pathway was not changed suggesting that clathrin-mediated endocytosis is selectively impaired by ethanol. To test this possibility, we examined the internalization of a panel of proteins and compounds internalized by different mechanisms in control and ethanol-treated WIF-B cells. We determined that the internalization of markers known to be internalized via clathrin-mediated mechanisms was impaired. In contrast, the internalization of markers for caveolae/raft-mediated endocytosis, fluid phase internalization or non-vesicle-mediated uptake was not impaired in ethanol-treated cells. We further determined that clathrin heavy chain accumulated at the basolateral surface in small puncta in ethanol-treated cells while there was decreased dynamin-2 membrane association. Interestingly, the internalization of resident apical proteins that lack any known internalization signals was also disrupted by ethanol suggesting that these proteins are internalized via clathrin-mediated mechanisms. This conclusion is consistent with our findings that dominant negative dynamin-2 overexpression impaired internalization of known clathrin markers and single spanning apical residents, but not of markers of fluid phase or raft-mediated internalization. Together these results indicate that ethanol exposure selectively impairs hepatic clathrin-mediated internalization by preventing vesicle fission from the plasma membrane.

Keywords

WIF-B cells; ethanol; liver injury; dynamin-2; endocytosis; clathrin

1. Introduction

Alcoholic liver disease is a major biomedical health concern in the United States. Despite considerable research efforts aimed at understanding the progression of the disease, the specific mechanisms leading to alcohol-induced damage remain elusive. Defining the alcohol-induced defects in protein trafficking is an active area of research in understanding hepatotoxicity. To

Corresponding Author: Pamela L. Tuma, PhD, Department of Biology, The Catholic University of America, 620 Michigan Avenue, NE, Washington, DC 20064, Tel. 202-319-6681, Fax. 202-319-5721, Email: tuma@cua.edu.

date, numerous proteins are known to have alcohol-induced alterations in their dynamics [1–5]. In general, two transport pathways appear to be affected: transport of newly-synthesized secretory or membrane proteins from the Golgi to the basolateral membrane and receptor-mediated endocytosis from the sinusoidal surface. Both impaired secretion and internalization require ethanol metabolism and are likely mediated by acetaldehyde [5,6].

Our recent studies on alcohol-induced defects in protein trafficking have been performed in WIF-B cells. These cells, when cultured on plastic or glass coverslips, enter a terminal differentiation program. After 7–10 days in culture, 70–95% of WIF-B cells become fully differentiated and exhibit phase-lucent structures that are functionally and compositionally analogous to the bile canaliculi (BC) [7]. Domain-specific membrane proteins are localized in WIF-B cells as they are in hepatocytes in situ (Fig. 2B) and liver-specific functions are maintained [8,9]. Importantly for these studies, WIF-B cells maintain the ability to metabolize ethanol using endogenous alcohol dehydrogenase (ADH) and cytochrome P4502E1 [10]. Like hepatocytes, ethanol-treated WIF-B cells display a reduced redox state and increased triglycerides [10]. Also like in isolated hepatocytes and *in situ*, clathrin-mediated endocytosis of asialoglycoprotein receptor (ASGP-R) is impaired in ethanol-treated WIF-B cells [5]. We further determined that this impairment required ethanol metabolism and was likely mediated by acetaldehyde [5]. Similarly, ethanol impaired the transcytosis of a single spanning apical resident, aminopeptidase (APN). For both ASGP-R and APN, the block in trafficking was internalization from the basolateral membrane. Interestingly, no changes in transcytosis of the glycophosphatidylinositol (GPI)-anchored protein, 5′nucleotidase (5′NT), were observed suggesting that ethanol-treatment differentially regulates internalization pathways. We further determined that albumin secretion was impaired in ethanol-treated cells consistent with results from *in situ* studies [5]. Thus, WIF-B cells faithfully recapitulate many of the reported alcohol-induced defects in protein trafficking and provide a good model for mechanistic studies of impaired protein dynamics.

An open question from our previous studies is why 5′NT internalization was not altered in ethanol-treated cells. One possibility is that internalization mechanisms are differentially impaired by ethanol metabolism. There are at least three major internalization routes in mammalian cells: clathrin-mediated, caveolae/raft-mediated and non-clathrin/non-raft mediated [11] that are characterized by specific molecular players, cargoes and regulators. In general, the receptors that displayed impaired endocytosis in ethanol-treated hepatocytes *in situ* (ASGP-R, EGF-R, and to a lesser extent, insulin receptor) [1–3,12,13] and in WIF-B cells (ASGP-R) [5] are internalized via clathrin-mediated pathways. Although the basolateral internalization mechanism for 5′NT has not been identified in hepatocytes, its GPI-anchor suggests it is internalized via a caveolae/raft-mediated pathway. Thus, we propose that ethanol selectively impairs clathrin-mediated internalization. To test this possibility, we monitored the basolateral internalization of selected proteins/compounds endocytosed by different mechanisms in control and ethanol-treated WIF-B cells.

2. Materials and methods

2.1 Reagents and Antibodies

F12 (Coon’s) medium, FITC-conjugated cholera toxin B (CTxB), Lucifer Yellow and flourescein diacetate were purchased from Sigma-Aldrich (St. Louis, MO). Transferrin receptor (Tf-R) monoclonal antibodies (CL071AP) were from Cedarlane Laboratories (Burlington, NC) clathrin heavy chain antibodies (Clone X22) were from Novus Biologicals (Littleton, CO) and antibodies against dynamin-2 were from BD Biosciences (San Jose, CA). Fetal bovine serum was from Gemini Bio-Products (Woodland, CA) and Hepes was from HyClone (Logan, Utah). Alexa-466 and -568-conjugated secondary antibodies were purchased from Invitrogen (Carlsbad, CA). Antibodies against dipeptidyl peptidase IV (DPP IV),

hemagglutinin (HA) and polymeric IgA-receptor (pIgA-R) were all kindly provided by Dr. Ann Hubbard (Johns Hopkins School of Medicine, Baltimore, MD). Recombinant adenoviruses encoding V5/His6 epitope-tagged full-length DPP IV or pIgA-R and full-length HA were also all provided by A. Hubbard and have been described in detail [14].

2.2 Cell culture, virus production and infection

WIF-B cells were grown in a humidified 7% CO_2 incubator at 37°C as described [7]. Briefly, cells were grown in F12 medium, pH 7.0, supplemented with 5% FBS, 10 μM hypoxanthine, 40 nM aminopterin and 1.6 μM thymidine. Cells were seeded onto glass coverslips at 1.3×10^4 cells/cm^2 and grown for 8–12 days until they reached maximum density and polarity. In general, cells were treated on day 7 with 50 mM ethanol in medium buffered with 10 mM Hepes, pH 7.0 for 72 h as described [10].

Recombinant adenoviruses encoding V5/His6 epitope-tagged DPP IV or V5/myc-tagged pIgA-R or untagged HA that were generated using the Cre-Lox system [14] were provided by Dr. A. Hubbard (Johns Hopkins University School of Medicine, Baltimore, MD). The tetracycline repressible dynamin wild type and K44A dominant negative recombinant adenoviruses were provided by Drs. S. Schmid and H. Damke (Scripps, La Jolla, CA). For alcohol studies, WIF-B cells were infected after 48 h of ethanol treatment for 60 min at 37°C as described [14]. The cells were washed with complete medium and incubated an additional 18–20 h in the continued absence or presence of ethanol to allow protein expression. For the dynamin mutant analysis, cells were coinfected for 30 min at 37°C with recombinant adenovirus particles encoding the tetracycline repressible transactivator and wildtype or K44A dominant negative dynamins under the control of the tetracycline responsive element. After washing, the cells were incubated an additional 18–24 h to allow dynamin expression. For triple infections, cells were simultaneously incubated for 30 min at 37°C with dynamin wildtype or mutant virus, the transactivator and virus encoding full length DPPIV or pIgA-R and allowed to express as above.

2.3 Immunofluorescence Microscopy

WIF-B cells were fixed on ice with chilled phosphate buffered saline (PBS) containing 4% paraformaldehyde for 1 min and permeabilized with ice-cold methanol for 10 min. Cells were processed for indirect immunofluorescence as described previously [9]. Alexa-conjugated secondary antibodies were used at 5 μg/ml. Cells were visualized by epifluorescence using an Olympus BX60 Fluorescence Microscope (OPELCO, Dulles, VA). Images were taken with a Coolsnap HQ2 digital camera (Photometrics, Tucson, AZ) and IPLabs image analysis software (Biovision, Exton, PA). Adobe Photoshop (Adobe Systems Inc., Mountain View, CA) was used to compile figures.

To quantitate the relative distributions of the membrane proteins, random fields from each slide were visualized by epifluorescence and digitized as described [15,16]. From micrographs, the average pixel intensity of selected regions of interest (ROI) placed at the apical or basolateral surface of the same WIF-B cell (for pIgA-R, DPP IV and HA) were measured using the Measure ROI tool of the ImageJ software (National Institutes of Health). For Tf-R, the average pixel intensity at recycling endosomes or plasma membrane of the same cell was measured. The averaged background pixel intensity was subtracted from each value and the ratio of apical to basolateral membrane (for pIgA-R, DPP IV and HA) or intracellular to basolateral membrane fluorescence intensity (for Tf-R) was determined.

2.4 Antibody trafficking in live cells

Cells were continuously labeled with anti-Tf-R antibodies (1:25) for 30 min at 37°C in complete medium. Cells were washed 3 times for 2 min each in chilled complete medium, were

fixed and labeled with Alexa-conjugated secondary antibodies. To monitor internalization of apical markers, cells were surface labelled with antibodies specific to DPPIV (1:50), APN (1:50) or pIgA-R (1:25) for 15–30 min at 4°C. Because tight junctions restrict access of the antibodies to the apical PM, only antigens at the basolateral surface were labeled. Cells were washed 3 times for 2 min on ice with chilled medium and then reincubated with prewarmed complete medium. Antibodies with bound antigens were chased for 45 or 90 min at 37°C. Cells were washed and processed as described above.

2.5 Cholera toxin internalization

Control or treated WIF-B cells were rinsed 3 times with prewarmed serum-free medium then continuously incubated with 0.5–1.0 μg/ml FITC-CTxB in complete serum-free medium for 60 min at 37°C. Cells were washed 3 times for 2 min each with PBS, fixed and visualized directly by epifluorescence. Intracellular vs. surface fluorescence intensities were measured as described above.

2.6 Lucifer Yellow and HRP internalization

Control or treated WIF-B cells were rinsed 3 times with prewarmed serum-free medium then continuously incubated with 1.0 mg/ml Lucifer Yellow in serum-free medium for 30 min at 37°C. After rinsing with prewarmed medium, live cells were imaged directly by epifluorescence. To quantitate amounts of Lucifer Yellow internalized, intracellular fluorescence was monitored using a plate reader. After internalization and washing, cells were scraped from coverslips in 100 μl PBS containing 0.1% Triton X-100, and 50 μl of each sample was placed in a 96-well dish. Flourescence was detected with the plate reader emission wavelength set at 428 nm and emission at 536 nm. Levels of internalized Lucifer Yellow were determined relative to a standard curve of known concentrations.

Control or dynamin expressing WIF-B cells were incubated for 2h with 5 mg/ml HRP at 37° C. Cells were washed 3 times for 2 min each with chilled medium, then fixed as described above and immunolabeled with anti-HRP antibodies. Cells were visualized by epifluorescence and images collected from random fields. From micrographs, dynamin expressing cells were scored for the absence or presence of intracellular HRP labeling and percent positive cells calculated.

2.7 Fluorescein diacetate labeling

Control or treated cells were rinsed 3 times with prewarmed complete medium then continuously incubated with 0.5 μg/ml fluorescein diacetate in complete medium for 20 min at 37°C. After rinsing with prewarmed medium, live cells were imaged directly by epifluorescence. To determine the percentage of bile canalicular (BC) structures labeled, random fields from each slide were visualized by epifluorescence or phase contrast and digitized. From phase micrographs, the total number of BCs was counted, and from the corresponding epifluorescence image, the number of labeled BCs was calculated (labeled BCs/ total BCs). High, medium and low fluorescence labeling intensities of BCs were also scored from the same micrographs.

2.8 Cell fractionation

WIF-B cells grown on 10 cm dishes were rinsed with PBS, detached with trypsin for 2 min at 37 °C and pelleted by centrifugation. Cells from two dishes were pooled, resuspended in 5 ml ice-cold swelling buffer (1 mM $MgCl_2$, 1 mM DTT, 1 mM EGTA) and incubated 5 min on ice. Cells were pelleted by centrifugation and resuspended in 500 μl of PEM (100 mM Pipes, 1 mM EGTA, 1 mM $MgSO_4$, pH 6.6) with added protease inhibitors (1 μg/ml each of leupeptin, antipain, PMSF and benzamidine) and Dounce-homogenized with a tight fitting pestle for 20

strokes. The homogenate was centrifuged for 60 min at 4°C at 150,000 × g to prepare cytosolic and total membrane fractions. The fractions proteins were immunoblotted for clathrin heavy chain and dynamin-2 and the relative distributions were determined by densitometry.

2.9 Statistical Analysis

Results were expressed as the mean ± S.E.M. Comparisons between control and ethanol-treated cells were made using the Student's *t* test for paired data. *P* values of ≤ 0.05 were considered significant.

3. Results

3.1 Ethanol impairs clathrin-mediated, but not caveolae/raft-mediated internalization

We first examined the steady state distributions of two well-characterized markers known to be constitutively internalized by clathrin-mediated endocytosis: transferrin receptor (Tf-R), a protein that recycles between the basolateral membrane and recycling endosomes in the presence or absence of ligand, and polymeric IgA-receptor (pIgA-R), a transcytosing protein that traverses the basolateral membrane en route to the canalicular surface. In control cells, the majority of Tf-R was present on intracellular, perinuclear structures corresponding to recycling endosomes (Fig. 1A, a) while pIgA-R mainly distributed to the apical membrane (Fig. 1A, c). In ethanol treated cells, a striking increase in staining at or near the basolateral membrane was observed for both markers (Fig. 1A, b and d). Such a shift in distribution is consistent with impaired receptor internalization.

To quantitate our morphological observations, we measured Tf-R and pIgA-R relative distributions from micrographs using our previously published method [15,16]. The fluorescence intensities of selected regions of interest placed at intracellular vs. basolateral populations of Tf-R or at apical vs. basolateral populations of pIgA-R were measured. The averaged background intensity was subtracted from each value and the ratio of intracellular to basolateral membrane (for Tf-R) or apical to basolateral membrane fluorescence intensity (for pIgA-R) was determined. For both receptors, their corresponding ratios were decreased to only ~40% of control values in ethanol treated cells indicating more receptors were present at the basolateral surface consistent with decreased internalization. These decreased values are consistent with those determined previously for ASGP-R in ethanol-treated WIF-B cells (56% of control) [5].

To confirm directly that clathrin-mediated internalization was impaired in ethanol treated cells, we monitored the trafficking of antibody-labeled Tf-R. Live cells were continuously labeled with antibodies specific to external receptor epitopes for 30 min. Cells were fixed and the trafficked antigen-antibody complexes were detected with secondary antibodies. In control cells, significant Tf-R populations were detected in intracellular structures (Fig. 1C a) with very little basolateral labeling indicating that Tf-R was rapidly internalized. In contrast, in ethanol-treated cells (Fig. 1C, b), Tf-R was mainly detected at the basolateral surface indicating that the increased Tf-R steady state basolateral staining was due to impaired internalization.

Our previous results showing that the internalization of the GPI-anchored protein, 5′NT, was not impaired in ethanol-treated cells suggested that caveolae/raft-mediated endocytosis was not altered by ethanol exposure. To test this hypothesis, we measured the internalization of FITC-conjugated cholera toxin B (CTxB). This subunit binds ganglioside M1, a known component of lipid rafts and is internalized via a caveolae/raft-mediated mechanism [17]. Once internalized, CTxB is delivered first to the Golgi and then to the ER [17]. As shown in Fig. 2A, there was no observable difference in CTxB internalization between control and ethanol-treated cells. In both cases, significant reticular ER-like staining was observed with some

labeling detected at the basolateral surface (Fig. 2A). When quantitated, the intracellular to basolateral fluorescence intensity ratios were virtually identical (Fig. 2B) indicating endocytosis was not impaired. Thus, we conclude that caveolae/raft-mediated internalization is not altered in ethanol-treated cells.

3.2 Ethanol does not impair fluid phase or non-vesicle-mediated internalization

To test whether fluid phase internalization is altered by ethanol treatment and to further confirm that WIF-B cells are a good model for studying mechanisms of hepatotoxicity, we monitored the internalization and lysosomal delivery of Lucifer Yellow in control and treated cells. As in isolated hepatocytes from ethanol-fed rats [18], no change in Lucifer Yellow internalization was observed in ethanol-treated cells (Fig. 3A). After 30 min of uptake, Lucifer Yellow was detected in large intracellular structures corresponding to lysosomes in both control and ethanol-treated cells (Fig. 3A). We confirmed these morphological results by measuring total intracellular fluorescence. After incubation with Lucifer Yellow for 30 min, cells were detached from coverslips by addition of PBS containing 1.0% Triton X-100. The lysates were placed in a 96-well dish and fluorescence detected with a plate reader. In general, robust Lucifer Yellow internalization was observed in both control and ethanol-treated cells (range: ~65–210 ng/coverslip) (Fig. 3B). These results confirm that fluid phase internalization was not altered in ethanol-treated WIF-B cells.

We also examined non-vesicle-mediated internalization in control and ethanol-treated cells by monitoring the uptake of the organic anion, fluorescein diacetate. Once internalized, this anion diffuses across the cell and is secreted from the canalicular surface. In both control and ethanol-treated WIF-B cells, fluorescein diacetate was detected in the BC-like structures (Fig. 4A) indicating efficient internalization and subsequent apical secretion. These morphological observations were confirmed when we quantitated BC fluorescence. Virtually no difference in the number of labeled BCs was observed between control and ethanol-treated cells (81.0 ± 3.6% vs. 78.7 ± 5.0, respectively). Similarly, when scored for fluorescence intensity, virtually identical proportions of labeled BCs exhibited low, medium or high fluorescence levels (Fig. 4B). Thus, non-vesicle-mediated internalization was not impaired in ethanol-treated cells. These results further indicate that canalicular secretion was not impaired upon ethanol exposure.

3.3 Clathrin coated assemblies accumulate at the plasma membrane in ethanol-treated cells

To more directly determine whether clathrin-mediated internalization was impaired by ethanol exposure, we examined the distributions of clathrin heavy chain, a major coat component of clathrin. In control cells, diffuse cytosolic and faint basolateral membrane staining was observed with significant labeling of intracellular structures (likely Golgi) (Fig. 5A, a). Although the intracellular and cytosolic labeling was detected in ethanol-treated cell, there was a striking increase in staining of clathrin heavy chain at the basolateral membrane (Fig. 5A, b) in discrete puncta (see inset) suggesting that clathrin-coated vesicle fission was impaired.

We next immunoblotted cytosolic and total membrane fractions prepared from control or ethanol-treated cells for clathrin heavy chain or dynamin-2. Importantly, this dynamin isoform has recently been shown to selectively regulate clathrin-mediated endocytosis; it is not required for cholera toxin, caveolae or raft-mediated internalization [20]. Furthermore, dynamin-2 is thought to function in late stages of vesicle formation and fission. Comparison of the whole homogenate (WH) samples revealed that the levels of neither clathrin heavy chain nor dynamin-2 were changed by ethanol treatment indicating that impaired clathrin-mediated internalization was not simply due to decreased protein amounts. Although membrane association of clathrin heavy chain was maintained in ethanol-treated cells, (81.7 ± 6.6 vs. 82.9 ± 5.3, control vs. ethanol, respectively), dynamin-2 membrane association was markedly

decreased (Fig. 5B). In control cells, over 70% (71.6 ± 5.3) of dynamin-2 is membrane-associated. In contrast, only ~50% (54.2 ± 2.9) of dynamin-2 associates with membranes in ethanol-treated cell. These results suggest that clathrin-coated assemblies are formed at the plasma membrane, but vesicle fission is impaired, and that the impaired fission is due to decreased membrane recruitment of dynamin-2. These findings are remarkably consistent with the increased basolateral staining observed for the markers of clathrin-mediated internalization.

3.4 Ethanol impairs the endocytosis of apical residents with no known internalization signals

In hepatocytes, newly synthesized single spanning resident apical proteins take an indirect route to the apical surface. They are transported from the *trans*-Golgi network (TGN) to the basolateral surface where they are selectively retrieved by endocytosis and transcytosed to the apical surface. However, unlike basolateral resident proteins, no specific targeting signal sequences have been identified that guide them along this circuitous pathway [19]. Our previous studies have also indicated that these apical residents are not internalized via caveolae/raft-mediated pathways [15]. Furthermore, the short cytoplasmic domains of the apical residents lack any known tyrosine- or dileucine-based clathrin-mediated internalization signal sequences [19]. Thus, our recent finding that the basolateral internalization of APN was impaired in ethanol-treated cells is intriguing [5].

To determine if internalization of other single spanning apical residents is impaired by ethanol exposure, we examined the steady state distributions of another ectoenzyme (dipeptidyl peptidase IV; DPP IV), and an exogenously expressed viral protein (hemagglutinin; HA) in control and treated cells. In control cells, both DPP IV and HA were present mainly at the apical surface (Fig. 6A, a and c). In contrast, a striking increase in staining at or near the basolateral membrane was observed for both markers in ethanol-treated cells (Fig. 6A, b and d). For both receptors, the apical to basolateral fluorescence intensity ratios were decreased in ethanol-treated cells (Fig. 6B). As for Tf-R and pIgA-R measurements, HA intensity ratio was 40% of that of control. Although the decreased ratio for DPP IV was less dramatic (80% of control), it was significant ($P < 0.02$).

To confirm directly that DPP IV internalization was impaired in ethanol-treated cells, we monitored the trafficking of a cohort of antibody-labeled DPP IV. Live cells were labeled with DPP IV antibodies specific to external epitopes at 4°C. After washing, the labeled DPP IV cohort was chased for 45 or 90 min at 37°C. Cells were fixed and labeled with secondary antibodies to detect the trafficked antigen-antibody complexes. In control cells, significant DPP IV staining was detected at the apical surface (Fig. 6C, a and c) indicating that DPP IV was rapidly internalized and transcytosed to the apical surface. In contrast, in ethanol-treated cells (Fig. 5C, b and d), basolateral DPP IV staining was observed with a reciprocal decrease in apical labeling. As for DDP IV at steady state, the apical to basolateral fluorescence intensity ratios were decreased, but to a much greater extent. After 45 min chase, the ratio was decreased to ~22% of control, and after 90 min, the ratio was ~30% of control. Thus, we conclude that the basolateral internalization of DPP IV was impaired in ethanol-treated cells.

Because the internalization of DPP IV and HA (and APN; [5]) was impaired to a similar extent as ASGP-R, pIgA-R and Tf-R, we suggest that these apical residents are endocytosed via clathrin-mediated pathways. To test this, we examined internalization of DPP IV and APN in cells expressing wildtype or dominant negative (K44A) dynamin-2. Importantly, this dynamin isoform has recently been shown to selectively regulate clathrin-mediated endocytosis; it is not required for cholera toxin, caveolae or raft-mediated internalization [20]. Overexpression of the dominant negative dynamin-2 induced remarkably similar defects in endocytosis as observed in ethanol-treated cells. In particular, the clathrin-mediated internalization of pIgA-R was drastically impaired. In cells overexpressing wild type dynamin-2, virtually all of the antibody-labeled receptor was chased to the apical surface (Fig. 7A, a). In contrast, in dynamin

K44A overexpressing cells, virtually no pIgA-R apical labeling was observed (marked with an asterisk) with a reciprocal increase in basolateral staining indicating impaired internalization (Fig. 7A, b). When pIgA-R distributions were quantitated as described above, the ratio of apical to basolateral fluorescence intensity was only 5% of control indicating a near complete block in internalization (Fig. 7B).

The internalization of DPP IV and APN was also impaired in cells expressing dominant negative dynamin-2. As for pIgA-R in dynamin wildtype expressing cells, the majority of DPPIV and APN antigen-antibody complexes were chased to the apical surface (Fig. 7A, c and e) while in dynamin K44A expressing cells, virtually no apical labeling was observed for DPPIV (unlabeled BCs are marked with asterisks) whereas decreased labeling was observed for APN (note the much brighter apical labeling in the BC of the adjacent, non-dynamin expressing cells) (Fig. 7A, d and f). As for pIgA-R, a reciprocal increase in basolateral labeling was observed in the dynamin K44A expressing cells (Fig. 7A, d and f). When quantitated, the apical to basoalteral fluorescence intensities for APN and DPP IV were ~20 and 40% of control levels, repectively, indicating impaired internalization.

To verify that dynamin-2 selectively impairs clathrin-mediated internalization in WIF-B cells, we monitored the internalization of markers of other endocytic pathways. Like in ethanol treated cells, neither the fluid phase internalization of HRP (Fig. 7A, g and h and Fig. 7B) nor the caveolae/raft-mediated internalization of CTxB (Fig. 7B) was changed by dynamin K44A expression (Fig. 7B). Together these results indicate that the single spanning apical residents are basolaterally internalized via a clathrin-mediated pathway.

4. Discussion

This study was initiated to determine whether clathrin-mediated endocytosis from the basolateral membrane is selectively impaired by ethanol exposure in polarized hepatic cells. To test this possibility, we examined endocytosis of a broad array of proteins and compounds that are known to be internalized by distinct mechanisms. As we hypothesized, the constitutive clathrin-mediated internalization of pIgA-R and Tf-R was significantly impaired in ethanol-treated WIF-B cells. In contrast, the caveolae/raft-mediated internalization of CTxB, the fluid phase uptake of Lucifer Yellow and the non-vesicle-mediated uptake of fluorescein diacetate were not impaired after ethanol exposure. Ethanol exposure led to the redistribution of clathrin heavy chain to puncta at the basolateral surface suggesting impaired vesicle fission. This conclusion is further substantiated by our findings that there is markedly less dyanmin-2 associated with membranes in ethanol-treated cells. These findings are strikingly consistent with the increased basolateral staining observed for the markers of clathrin-mediated internalization. Interestingly, the internalization of single spanning apical membrane residents that contain no known internalization signaling information was significantly impaired suggesting these proteins may be endocytosed by a clathrin-mediated mechanism. This was confirmed in cells expressing dominant negative dynamin-2.

4.1 Impact of impaired clathrin-mediated internalization on liver function

Endocytosis serves as the interface between the hepatocyte and its external environment and is critical for intercellular communication and signal transduction. Endocytosis also functions to retrieve metabolites from the blood such that small impairments can lead to increased levels of circulating hormones, growth factors, cytokines and other ligands. This is consistent with reports where increased levels of circulating interleukin-6, transferrin and pIgA were observed in ethanol-fed rats [21–24]. These results also are remarkably consistent with the observed defects in pIgA-R and Tf-R internalization reported here. Because these and other ligands are all associated with specific biological responses, small defects in their endocytosis can lead to alterations in hepatic homeostasis and metabolism which can promote liver injury. Thus,

defining the mechanisms responsible for impaired clathrin-mediated endocytosis in ethanol-treated hepatocytes may have important clinical implications.

4.2 Mechanism of alcohol-induced impairment of clathrin-mediated internalization

At present, the specific mechanisms responsible for ethanol-induced defects in clathrin-mediated internalization are not known. Because the clathrin-mediated internalization of many unrelated proteins was impaired *in situ*, in isolated hepatocytes and in ethanol-treated WIF-B cells, we believe that it is a universal regulator of clathrin-mediated internalization that is impaired, *not* the receptors themselves. Previously, we determined that microtubule hyperacetylation induced by ethanol or by addition of a tubulin deacetylase inhibitor correlated with impaired clathrin-mediated endocytosis [5]. Because impaired ASGP-R clathrin-mediated internalization required ethanol metabolism and was likely mediated by acetaldehyde [5], another exciting possibility is that the molecular machinery that drives clathrin-mediated endocytosis is more prone to adduction by acetaldehyde or other reactive metabolites than the molecules regulating other internalization routes. Such adduction could lead to the increased basolateral associations of the clathrin coat components, defective receptor or dynamin-2 recruitment. We are currently exploring these and other possibilities.

4.4 Are alcohol-induced defects in clathrin-mediated internalization and secretion related?

Previously it has been demonstrated that alcohol induced impaired transport of newly synthesized glycoproteins from the Golgi to the basolateral membrane in hepatocytes *in situ* [3,25–27]. Although the identities of these proteins were not defined, it is intriguing to note that basolateral resident proteins contain targeting information that likely promotes their recruitment into clathrin-coated vesicles at the TGN [28]. These basolateral targeting signals are similar to the signals required for clathrin-internalization and are either tyrosine-based or contain a di-leucine motif [28]. Thus, one exciting possibility is that an alcohol-induced modification of the clathrin machinery also leads to defective vesicle fission at the TGN. Although constitutive secretory proteins are thought to bud from the TGN in different vesicle populations than transmembrane proteins [29], it is not yet clear what factors are required for their formation. Because constitutive secretion is also impaired in ethanol-treated hepatic cells, one possibility is that at least some components of the clathrin machinery are shared, and that these components are readily modified by reactive alcohol metabolites. Clearly, this is a fertile area of investigation for future research.

4.3 Are single spanning apical proteins internalized via clathrin-mediated mechanisms?

In hepatocytes, newly synthesized single spanning apical resident proteins take the “indirect” route to the canalicular surface. They are transported from the TGN to the basolateral surface where they are retrieved by endocytosis and transcytosed to the apical surface [19]. Currently, little is known about how apical proteins are selectively retrieved from the basolateral membrane. Our previous studies indicated that they are not likely internalized via caveolae/raft-mediated pathways [15]. When cholesterol or glycosphingolipids (raft components) were depleted from WIF-B cells, internalization was not changed. Furthermore, the short cytoplasmic domains (6–12 amino acids) of the apical residents lack any known tyrosine- or dileucine-based clathrin-mediated internalization signal sequences [19]. However, our finding that internalization of DPP IV, HA and APN were all impaired to a similar extent as ASGP-R, pIgA-R and Tf-R suggest that apical residents may be endocytosed via clathrin-mediated pathways. This is supported by our observation that overexpressed dominant negative dynamin-2 impaired internalization of pIgA-R, ASGP-R, DPP IV and APN, but not internalization of CTxB or HRP. However it remains to be determined whether the apical residents are actively recruited to clathrin-coated vesicles or if they are passive passengers.

Acknowledgments

We thank Dr. Ann Hubbard for providing many antibodies and viruses used in this study. We thank Drs. Hanna Damke and Sandra Schmid for supplying the dynamin viruses. This project was funded by the National Institute of Health grant AA015683 awarded to P.L.T.

List of Abbreviations

5′NT
: 5′nucleotidase

APN
: aminopeptidase N

ASGP-R
: asialoglycoprotein receptor

BC
: bile canaliculus

CTxB
: cholera toxin B subunit

DPP IV
: dipeptidyl peptidase IV

GPI
: glycophosphatidylinositol

HA
: hemagglutinin

pIgA-R
: polymeric IgA receptor

Tf-R
: transferrin receptor

TGN
: *trans*-Golgi network

References

1. Tuma DJ, Casey CA, Sorrell MF. Effects of ethanol on hepatic protein trafficking: impairment of receptor-mediated endocytosis. Alcohol Alcohol 1990;25:117–25. [PubMed: 2165408]
2. Tuma DJ, Casey CA, Sorrell MF. Effects of alcohol on hepatic protein metabolism and trafficking. Alcohol Alcohol Suppl 1991;1:297–303. [PubMed: 1669008]
3. Tuma DJ, Sorrell MF. Effects of ethanol on protein trafficking in the liver. Semin Liver Dis 1988;8:69–80. [PubMed: 3283943]
4. McVicker BL, Casey CA. Effects of ethanol on receptor-mediated endocytosis in the liver. Alcohol 1999;19:255–60. [PubMed: 10580516]
5. Joseph RA, Shepard BD, Kannarkat GT, Rutledge TM, Tuma DJ, Tuma PL. Microtubule acetylation and stability may explain alcohol-induced alterations in hepatic protein trafficking. Hepatology 2008;47:1745–53. [PubMed: 18161881]
6. Clemens DL, Casey CA, Sorrell MF, Tuma DJ. Ethanol oxidation mediates impaired hepatic receptor-mediated enocytosis. Alcohol Clin Exp Res 1998;22:778–9. [PubMed: 9660299]

7. Shanks MR, Cassio D, Lecoq O, Hubbard AL. An improved polarized rat hepatoma hybrid cell line. Generation and comparison with its hepatoma relatives and hepatocytes in vivo. J Cell Sci 1994;107 (Pt 4):813–25. [PubMed: 8056838]
8. Griffo G, Hamon-Benais C, Angrand PO, Fox M, West L, Lecoq O, et al. HNF4 and HNF1 as well as a panel of hepatic functions are extinguished and reexpressed in parallel in chromosomally reduced rat hepatoma-human fibroblast hybrids. J Cell Biol 1993;121:887–98. [PubMed: 8491780]
9. Ihrke G, Neufeld EB, Meads T, Shanks MR, Cassio D, Laurent M, et al. WIF-B cells: an in vitro model for studies of hepatocyte polarity. J Cell Biol 1993;123:1761–75. [PubMed: 7506266]
10. Schaffert CS, Todero SL, McVicker BL, Tuma PL, Sorrell MF, Tuma DJ. WIF-B cells as a model for alcohol-induced hepatocyte injury. Biochem Pharmacol 2004;67:2167–74. [PubMed: 15135311]
11. Conner SD, Schmid SL. Regulated portals of entry into the cell. Nature 2003;422:37–44. [PubMed: 12621426]
12. Tuma DJ, Casey CA, Sorrell MF. Chronic ethanol-induced impairments in receptor-mediated endocytosis of insulin in rat hepatocytes. Alcohol Clin Exp Res 1991;15:808–13. [PubMed: 1755513]
13. Dalke DD, Sorrell MF, Casey CA, Tuma DJ. Chronic ethanol administration impairs receptor-mediated endocytosis of epidermal growth factor by rat hepatocytes. Hepatology 1990;12:1085–91. [PubMed: 2227804]
14. Bastaki M, Braiterman LT, Johns DC, Chen YH, Hubbard AL. Absence of direct delivery for single transmembrane apical proteins or their “Secretory” forms in polarized hepatic cells. Mol Biol Cell 2002;13:225–37. [PubMed: 11809835]
15. Nyasae LK, Hubbard AL, Tuma PL. Transcytotic efflux from early endosomes is dependent on cholesterol and glycosphingolipids in polarized hepatic cells. Mol Biol Cell 2003;14:2689–705. [PubMed: 12857857]
16. Ramnarayanan SP, Cheng CA, Bastaki M, Tuma PL. Exogenous MAL reroutes selected hepatic apical proteins into the direct pathway in WIF-B cells. Mol Biol Cell 2007;18:2707–15. [PubMed: 17494867]
17. Geny B, Popoff MR. Bacterial protein toxins and lipids: pore formation or toxin entry into cells. Biol Cell 2006;98:667–78. [PubMed: 17042742]
18. Casey CA, Camacho KB, Tuma DJ. The effects of chronic ethanol administration on the rates of internalization of various ligands during hepatic endocytosis. Biochim Biophys Acta 1992;1134:96–104. [PubMed: 1554752]
19. Tuma PL, Hubbard AL. Transcytosis: crossing cellular barriers. Physiol Rev 2003;83:871–932. [PubMed: 12843411]
20. Liu YW, Surka MC, Schroeter T, Lukiyanchuk V, Schmid SL. Isoform and splice-variant specific functions of dynamin-2 revealed by analysis of conditional knock-out cells. Mol Biol Cell 2008;19:5347–59. [PubMed: 18923138]
21. Hoek JB, Pastorino JG. Ethanol, oxidative stress, and cytokine-induced liver cell injury. Alcohol 2002;27:63–8. [PubMed: 12062639]
22. Hoek JB, Pastorino JG. Cellular signaling mechanisms in alcohol-induced liver damage. Semin Liver Dis 2004;24:257–72. [PubMed: 15349804]
23. Potter BJ, Chapman RW, Nunes RM, Sorrentino D, Sherlock S. Transferrin metabolism in alcoholic liver disease. Hepatology 1985;5:714–21. [PubMed: 4029886]
24. van de Wiel A, Delacroix DL, van Hattum J, Schuurman HJ, Kater L. Characteristics of serum IgA and liver IgA deposits in alcoholic liver disease. Hepatology 1987;7:95–9. [PubMed: 3542782]
25. Volentine GD, Ogden KA, Kortje DK, Tuma DJ, Sorrell MF. Role of acetaldehyde in the ethanol-induced impairment of hepatic glycoprotein secretion in the rat in vivo. Hepatology 1987;7:490–5. [PubMed: 3570159]
26. Volentine GD, Tuma DJ, Sorrell MF. Subcellular location of secretory proteins retained in the liver during the ethanol-induced inhibition of hepatic protein secretion in the rat. Gastroenterology 1986;90:158–65. [PubMed: 3940242]
27. Volentine GD, Tuma DJ, Sorrell MF. Acute effects of ethanol on hepatic glycoprotein secretion in the rat in vivo. Gastroenterology 1984;86:225–9. [PubMed: 6690349]
28. Rodriguez-Boulan E, Musch A. Protein sorting in the Golgi complex: shifting paradigms. Biochim Biophys Acta 2005;1744:455–64. [PubMed: 15927284]

29. Saucan L, Palade GE. Differential colchicine effects on the transport of membrane and secretory proteins in rat hepatocytes in vivo: bipolar secretion of albumin. Hepatology 1992;15:714–21. [PubMed: 1551647]

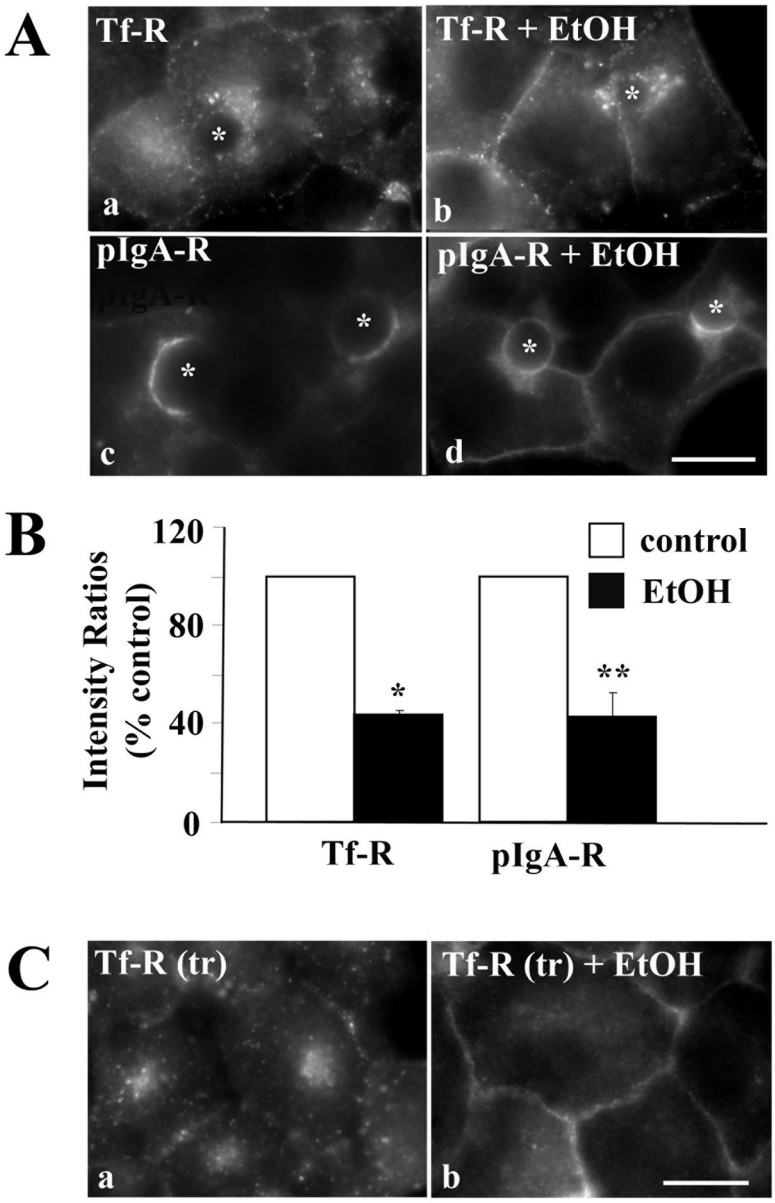

Figure 1.

Clathrin-mediated internalization is impaired in ethanol-treated cells. **A,** WIF-B cells were treated in the absence (a, c) or presence (b, d) of ethanol (EtOH) and labeled for Tf-R (a, b) or pIgA-R (c, d). Asterisks are marking selected BCs. **B,** WIF-B cells were treated as described in A. Random fields were visualized by epifluorescence and digitized. From micrographs, the average pixel intensity of each marker at selected regions of interest placed at the apical or basolateral membrane (for pIgA-R) or at the intracellular population and basolateral membrane (for Tf-R) of the same WIF-B cell was measured. The averaged background pixel intensity was subtracted from each value and the ratio of apical to basolateral or intracellular to basolateral fluorescence intensity was determined. In all cases, control ratios were set to 100%. Values are expressed as the mean ±SEM. Measurements were done on at least three independent experiments. * $P < 0.0005$, ** $P < 0.03$ **C,** Cells were treated in the absence (a) or presence (b) of ethanol (EtOH). Live cells were continuously labeled with anti-Tf-R antibodies for 30 min in the continued absence or presence ethanol. Cells were fixed,

permeabilized and labeled with secondary antibodies to detect the trafficked (tr) antibody-antigen complexes. Bar = 10 μm

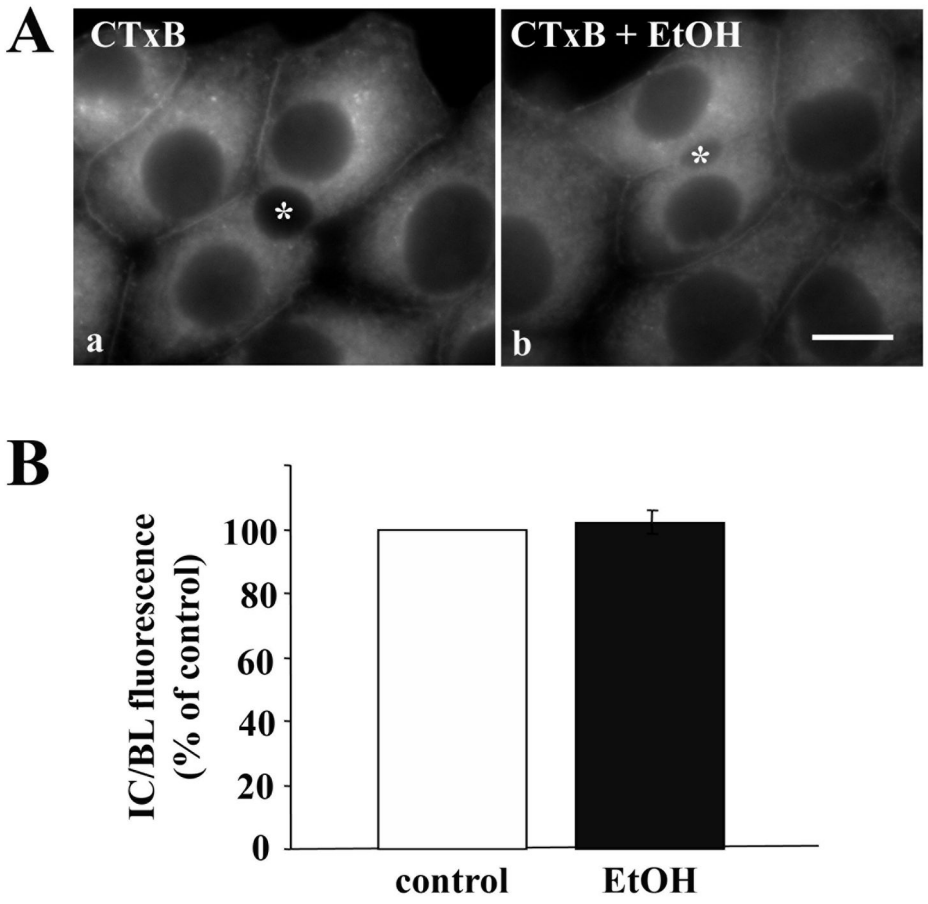

Figure 2.

Caveolae/raft-mediated internalization is not impaired in ethanol-treated cells. **A,** WIF-B cells were treated in the absence (a) or presence (b) of ethanol (EtOH). Cells were continuously labeled for 60 min at 37°C with 0.5 μg/ml CTxB. Cells were fixed and CTxB was visualized directly by epifluorescence. Asterisks are marking selected BCs. Bar = 10 μm **B,** The relative distributions of CTxB in control or ethanol-treated cells were quantitated as described in Figure 1B. Values are expressed as the mean ±SEM. Measurements were done on three independent experiments.

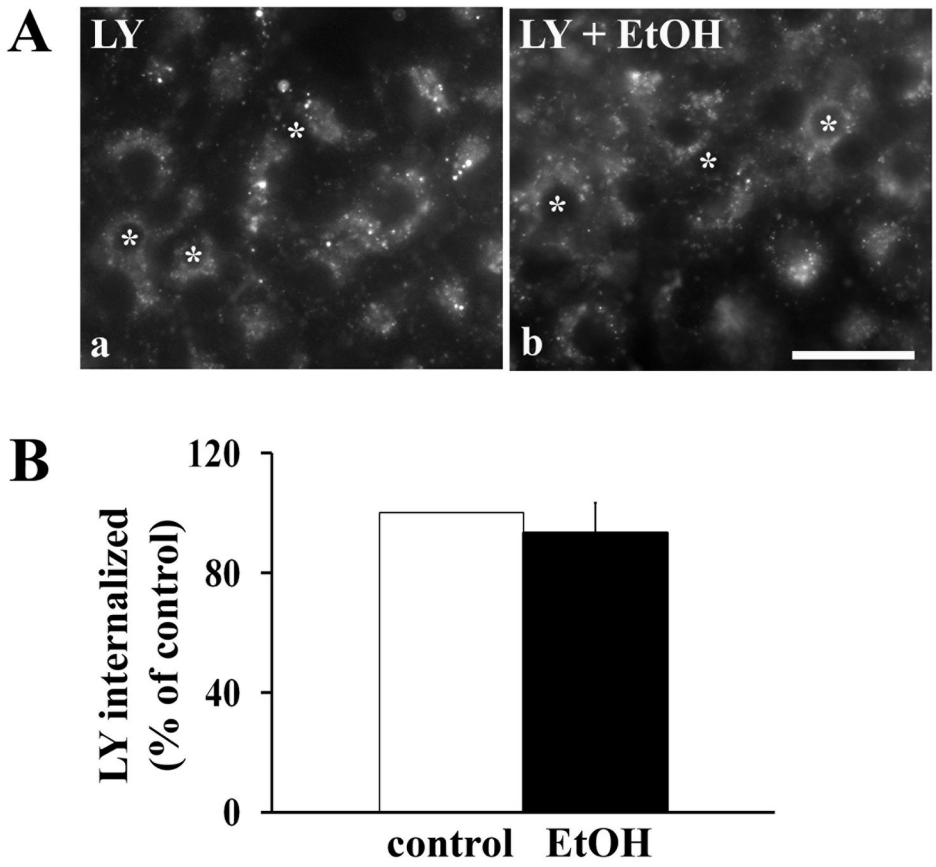

Figure 3.

Fluid phase endocytosis is not impaired in ethanol-treated cells. **A,** WIF-B cells were treated in the absence (a) or presence (b) of ethanol (EtOH). Cells were continuously labeled for 30 min at 37°C with 1.0 mg/ml Lucifer Yellow (LY). Cells were washed and live cells were visualized immediately by epifluorescence. Bar = 10 μm **B,** Control or ethanol-treated cells were continuously labeled for 30 min at 37°C with 2.0 mg/ml Lucifer Yellow (LY). Cells were detached from coverslips by addition of PBS containing 0.1% Triton X-100. The lysates were placed in a 96-well dish and fluorescence detected with a plate reader set at 428 nm excitation and 536 nm emission. Values are expressed as the mean ±SEM. Measurements were done on four independent experiments.

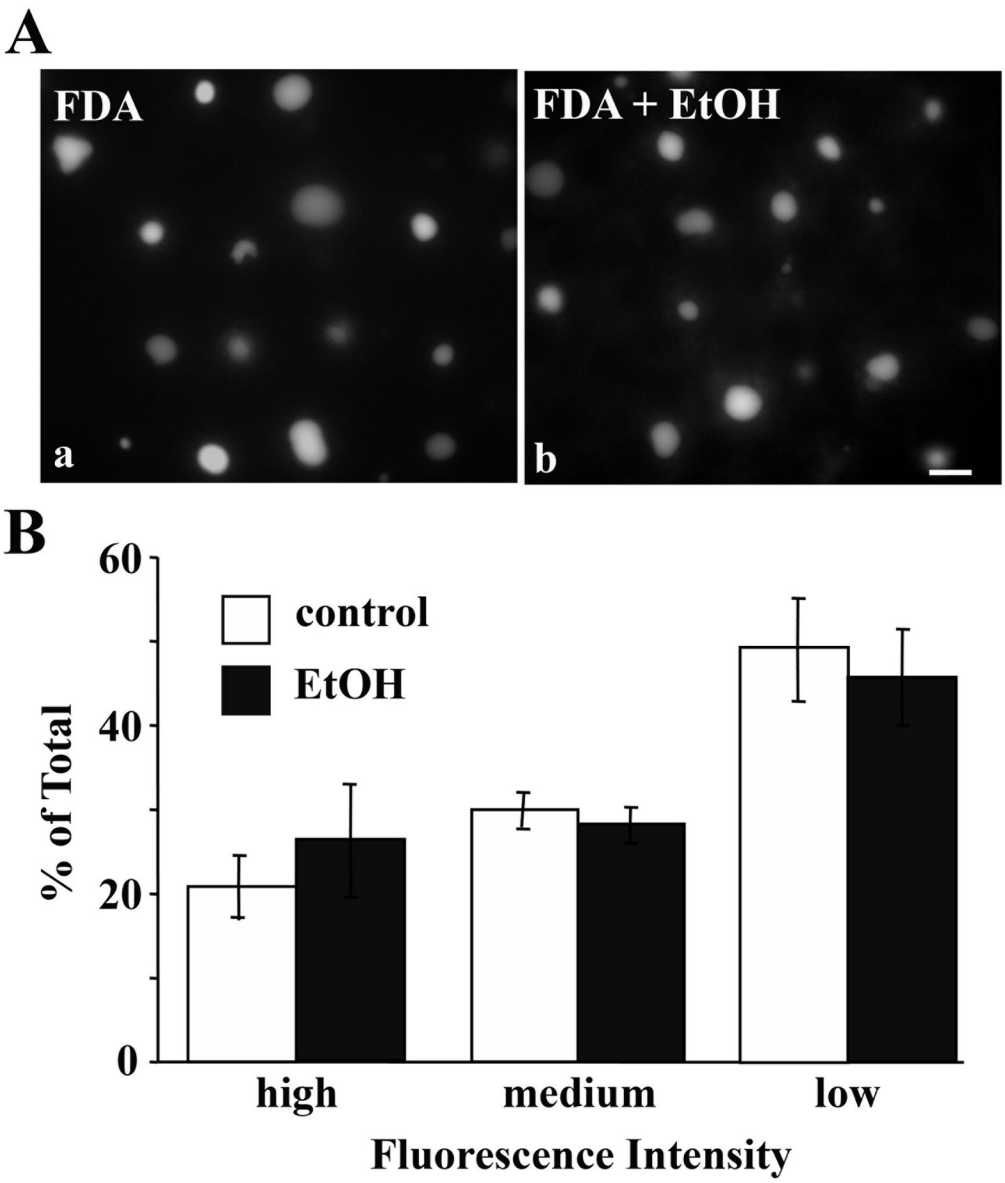

Figure 4.

The non-vesicle-mediated uptake and subsequent canalicular delivery of fluorescein diacetate is not altered in ethanol-treated cells. **A,** WIF-B cells were treated in the absence (a) or presence (b) of ethanol (EtOH). Cells were continuously labeled for 20 min at 37°C with 0.5 μg/ml fluorescein diacetate (FDA). Cells were washed and live cells were visualized immediately by epifluorescence. Bar = 10 μm **B,** Labeled BCs were scored for low, medium or high fluorescence intensity and the percentages plotted. Values are expressed as the mean ±SEM. Measurements were done on three independent experiments.

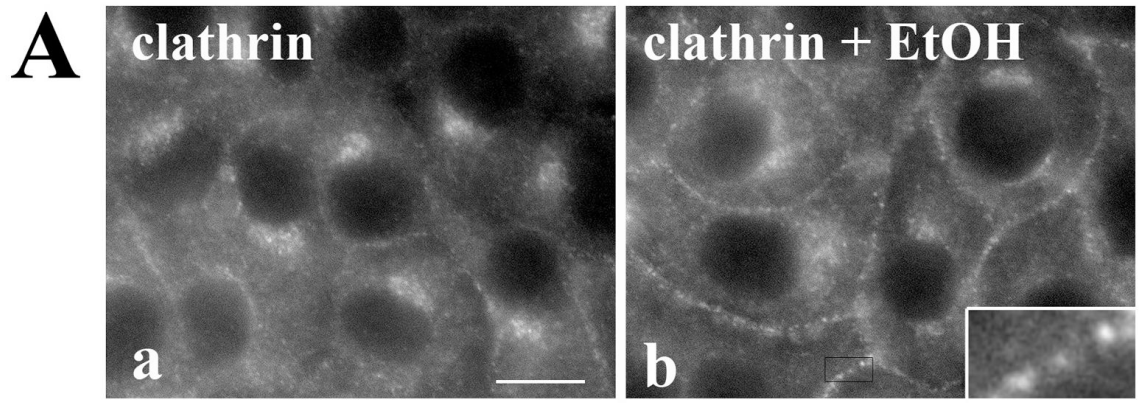

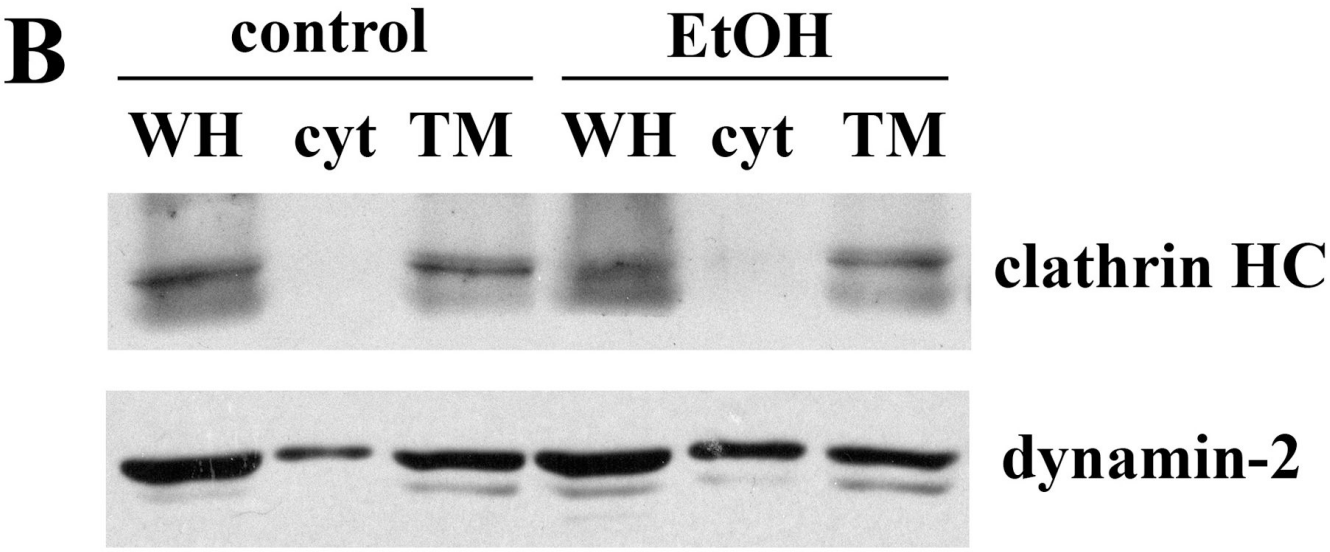

Figure 5.

Clathrin coated assemblies accumulate at the plasma membrane in ethanol-treated cells. **A,** WIF-B cells were treated in the absence (a) or presence (b) of ethanol (EtOH) and labeled for clathrin heavy chain. The inset is an enlarged image of the indicated boxed-in area. Bar = 10 μm **B,** Whole homogenate (WH), cytosolic (cyt) and total membrane (TM) fractions were prepared from control or ethanol-treated WIF-B cells and immunoblotted for clathrin heavy chain or dynamin-2 as indicated. The blots shown are representative of five independent experiments.

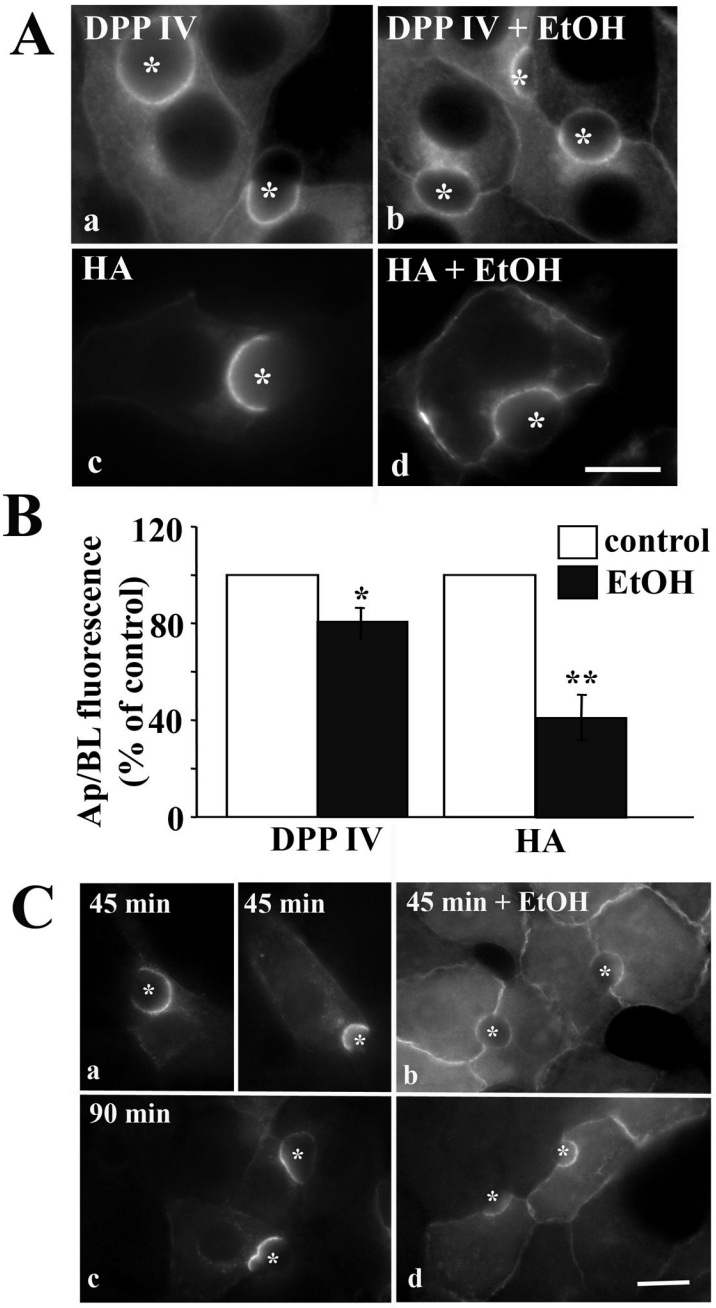

Figure 6.

Internalization of single spanning apical proteins with no known sorting information is impaired in ethanol-treated cells. **A,** WIF-B cells were treated in the absence (a, c) or presence (b, d) of ethanol (EtOH) and labeled for DPP IV (a, b) or HA (c, d). Asterisks are marking selected BCs. Bar = 10 μm **B,** WIF-B cells were treated as described in A and the relative distributions determined as described in Figure 1B. Values are expressed as the mean ±SEM. Measurements were done on at least three independent experiments. * $P < 0.05$; ** $P < 0.01$ **C,** Cells were treated in the absence (a) or presence (b) of ethanol (EtOH). Live cells were labeled with anti-DPP IV antibodies and the antigen-antibody complexes were chased for 45

or 90 min in the continued absence or presence ethanol. Cells were labeled with secondary antibodies to detect the trafficked (tr) complexes. Bar = 10 μm

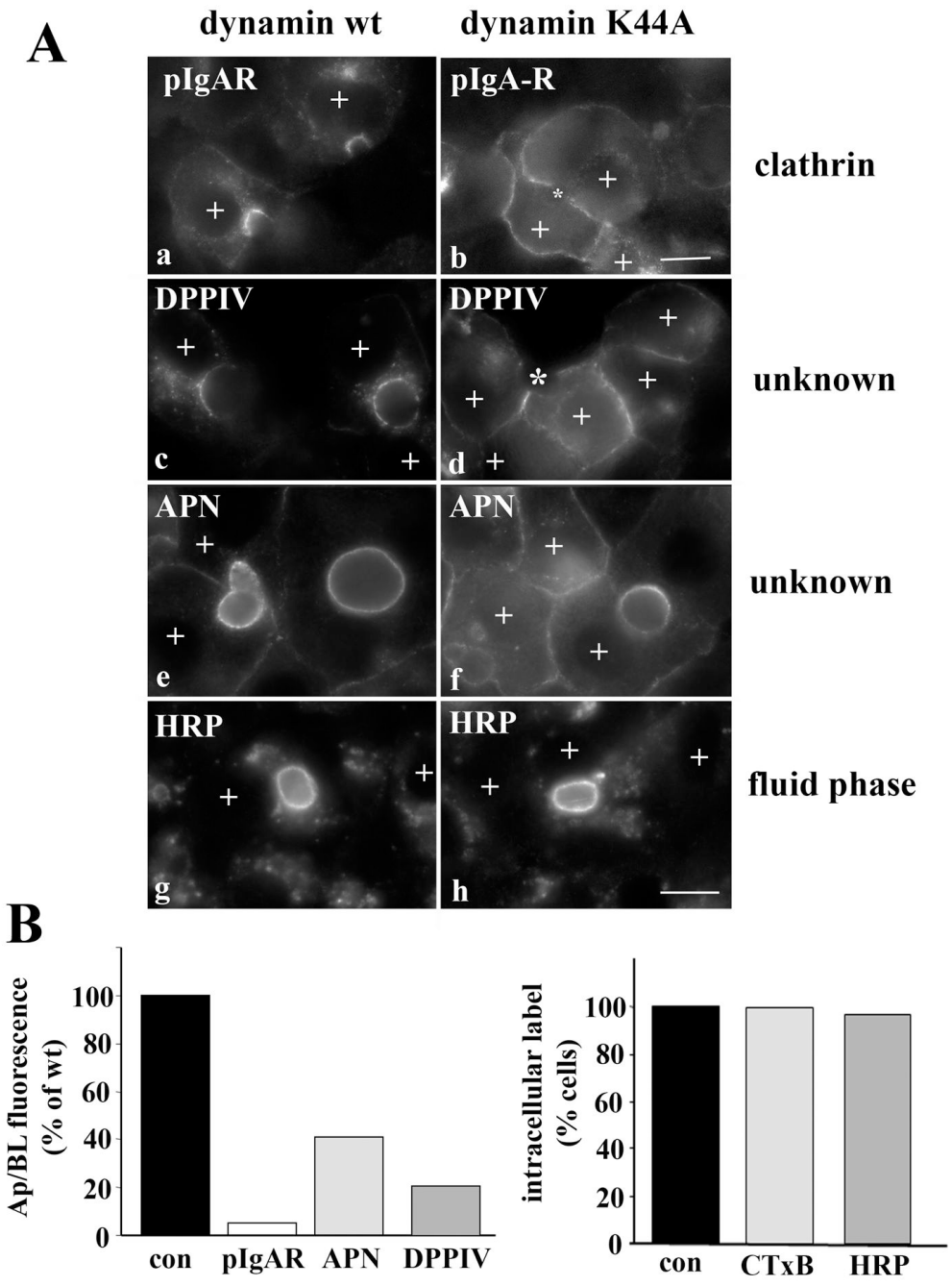

Figure 7.

Internalization of the single spanning apical residents is clathrin-dependent. A, WIF-B cells were co-infected for 30 min at 37°C with recombinant adenovirus particles encoding the tetracycline repressible transactivator and wildtype (a, c, e and g) or K44A dominant negative dynamins (b, d, f, and h) under the control of the tetracycline responsive element. Cells were additionally infected with pIgA-R (a and b) or DPPIV (c and d) viruses. After washing, the cells were incubated an additional 18–24 h to allow dynamin expression. Live cells were labeled with anti-pIgA-R (a and b), anti-DPP IV (c and d) or anti-APN (e and f) antibodies and the antigen-antibody complexes chased for 90 min. Cells were also continuously labeled for 2 h with 5 mg/ml HRP in serum free medium (g and h). Cells expressing the recombinant dynamin

adenoviruses are indicated with a "+" symbol. Asterisks in panels b and d are marking unlabeled BCs in cells overexpressing dynamin K44A. Bar = 10 μm B, Cells were infected with wild type of K44A dynamin viruses as described in A, and internalization of the indicated markers was monitored by epifluorescence. Apical to basolateral fluorescence intensities were measured for pIgA-R, DPPIV and APN in dynamin expressing cells as described in Figure 1A. For CTxB and HRP, dynamin-expressing cells were scored for the presence of labeled intracellular puncta, and percent positive cells calculated.